Critical exponents and amplitudes of the ferromagnetic transition in $La_{0.1}Ba_{0.9}VS_3$

R. Cabassi,[1,*] F. Bolzoni,[1] A. Gauzzi,[1,2] and F. Licci[1]
[1]*Istituto IMEM-CNR, Area delle Scienze, 43100 Parma, Italy*
[2]*Institut de Minéralogie et de Physique des Milieux Condensés, Université Pierre et Marie Curie—Paris 6, 140, rue de Lourmel, 75015 Paris, France*
(Received 5 September 2006; published 21 November 2006)

To study the origin of the magnetic transition in $BaVS_3$, we measured the dc magnetization on $La_{0.1}Ba_{0.9}VS_3$ sintered samples near the ferromagnetic transition. Effective critical exponents and amplitudes are obtained by means of standard modified Arrot plots and the Kouvel-Fisher method, while asymptotic critical exponents and amplitudes are obtained by means of "correction to scaling" analysis. The two methods yield similar results, but the latter is superior with respect to the achieved uncertainty. The obtained results indicate that the universality class of magnetic interactions driving the transition changes from short to long range when cooling through T_c.

DOI: 10.1103/PhysRevB.74.184425 PACS number(s): 75.40.Cx, 71.27.+a, 75.10.Hk, 75.10.Jm

I. INTRODUCTION

Critical exponent analysis in the vicinity of a second-order phase transition is known to be a powerful tool to single out the relevant microscopic interaction responsible for the transition.[1] Thanks to the underlying theory based on the scaling principle, this analysis can provide insights into the effective Hamiltonian driving the transition and the dimensionality of the system. This approach is particularly helpful in the study of strongly correlated systems, where the coexistence of diverse interactions and the inadequacy of simple models often prevent a satisfactory physical description.

In this work, we determine the critical exponents and amplitudes of the ferromagnetic transition at $\simeq 19$ K in $La_{0.1}Ba_{0.9}VS_3$, where La doping turns out to stabilize the transition. The results of this analysis can be a further tool in the study of the still controversial phase diagram of the $BaVS_{3-\delta}$ system. The latter has recently raised a great deal of attention, for it is a prototype of a magnetically frustrated $3d^1$ ($S=1/2$) strongly correlated electron system exhibiting a crossover from antiferro- (AF) to ferromagnetism (FM) depending upon sulfur deficiency δ. Magnetic frustration arises from the triangular lattice of chains of VS_6 octahedra along the c axis of the hexagonal crystal structure.[2] It has been established that, at $T_{MI}=69$ K, AF correlations among V $3d$ states open a spin gap, concomitant with a metal-insulator (MI) transition and suppressed by pressure at 2 GPa.[3] It has been proposed[4,5] that at $T<T_{MI}$ a spin-orbital liquid develops, with spin and orbital short-range order. In nearly stoichiometric samples with $\delta \approx 0$, at 30 K, a long-range incommensurate AF order is formed in the ab plane.[6] Instead, in sulfur-deficient samples with $\delta \geqslant 0.1$, a FM order with Curie temperature $T_C \approx 15$ K appears, as reported by Massenet *et al.*[7] The AF-FM crossover was explained in terms of the Hund interaction between extra electrons released by the sulfur vacancies and V $3d$ electrons that form the $3d^1$ configuration in the stoichiometric compound.[7,8] The origin of the MI transition, the magnetic ordering phenomena at lower temperature, the incommensurability of the AF structure, the reduced magnetic moments experimentally measured ($0.4\ \mu_B$/V),[6,8] and the anisotropy of the electronic correlations remain open questions that would require further experimental and theoretical work to understand the electronic correlations in $BaVS_{3-\delta}$. More recent works reported that a one-dimensional charge instability of the chains is concomitant with the occurrence of the MI transition.[9,10] Thus it was argued that such charge instability is the driving force of the transition. On the other hand, it has been established that both the electronic structure[11] and the transport properties are modestly anisotropic.[4] Whangboo *et al.*[12] proposed a model to explain these puzzling properties in terms of broken-symmetry electronic state in which pairs of nonmagnetic V atoms alternate with pairs of magnetic V atoms in each VS_6 chain. Jiang *et al.*[13] performed density functional theory (DFT) calculations on a model based on next-neighbor Heinsenberg interaction, obtaining a magnetic structure with intrachain ferromagnetic spin arrangement and interchain antiferromagnetic spin arrangement. The structure of $BaVS_3$ has been investigated by means of x-ray-diffraction analysis[14] which revealed a sequence of structural transitions, and there has been proposed a model for the $T<T_{MI}$ phases with a superstructure of *Im* symmetry having four inequivalent vanadium atoms per unit cell, with the appearing of strong distorsion in the VS_6 octahedra at $T<T_C$ which results in charge ordering along the V chains. To shed more light on this peculiar compound, here we investigate the nature and dimensionality of the magnetic interaction responsible for the ferromagnetic transition in $BaVS_3$ by means of a detailed critical exponent analysis near the critical temperature T_C. Hitherto, the ferromagnetic state has been little studied in this system and no critical exponent studies are available yet. Given the sensitivity of the magnetic properties on sulfur deficiency, we studied the 10% La-doped sample. We found that this substitution stabilizes the ferromagnetic phase, similarly to the case of sulfur vacancies. Indeed, also the three-valent La cation introduces extra electrons to the V $3d^1$ electronic configuration. As a result, the ferromagnetic transition of La-doped samples is sharper. We show that this factor, together with the high-quality $M(H)$ data, characterized by a temperature stability of 0.01 K, enables us to extract the values of the critical exponents amplitudes precisely and reliably.

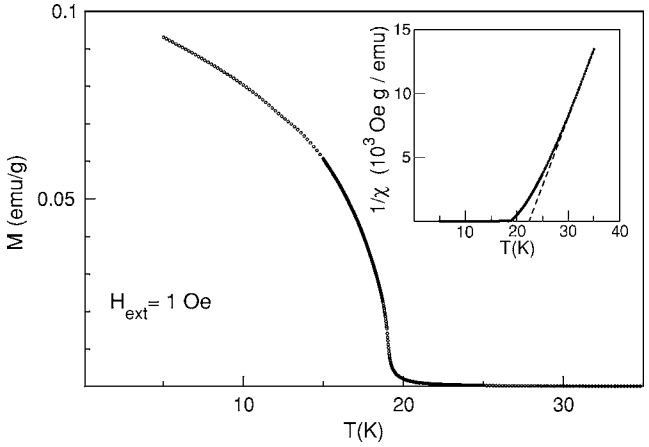

FIG. 1. Magnetization curve of $La_{0.1}Ba_{0.9}VS_3$ in applied external field $H=1$ Oe. Temperature steps are $\Delta T=0.02$ K inside the range 15–25 K, $\Delta T=0.2$ K outside. Inset: from $1/\chi$ vs T curve, one has $\mu_0=1.46\mu_B$ (dashed line).

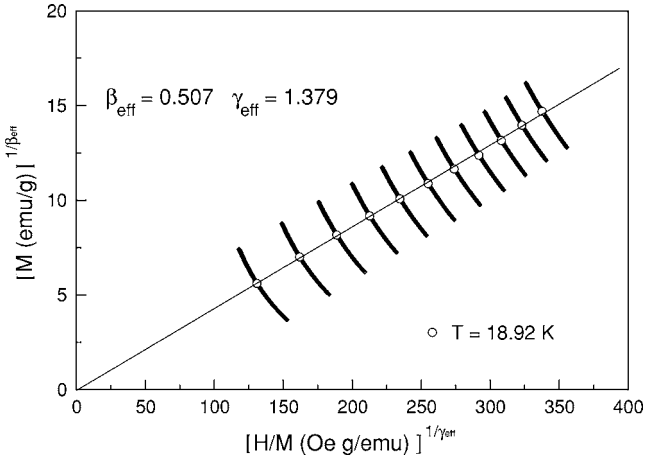

FIG. 2. Modified Arrot plots in the critical region $18.00 \leqslant T \leqslant 19.98$ K, with the β_{eff} and γ_{eff} values for which the best linear isotherms are obtained. The isotherm passing through the origin gives $T_C=18.92$ K. Points outside the range $0.1T<H<1.3T$ (not shown) have been excluded from the analysis (see text).

II. EXPERIMENT

The $La_{0.1}Ba_{0.9}VS_3$ sintered sample was prepared using a standard solid-state reaction route, as described elsewhere.[7] Neutron and x-ray diffraction revealed no secondary phases, except for traces of unreacted sulfur. In summary, Rietveld refinement of the diffraction data show that the sulfur deficiency, if any, is below the experimental error, $\delta \leqslant 0.02$. Magnetic measurements were performed using a commercial radio-frequency superconducting quantum interference device magnetometer. The studied sample exhibits the characteristic paramagnetic behavior of the undoped samples followed by a sharp ferromagnetic transition at $T_C \approx 19$ K (Fig. 1), with the paramagnetic slope of $\chi^{-1}(T)$ yielding an effective magnetic moment per V atom $\mu_0=1.46\mu_B$ (see the inset in Fig. 1). The measured value for T_C falls in the 15–20-K range of T_C values reported for sulfur-deficient undoped samples and the obtained value for μ_0 (comparable with the expected value $\mu_0=1.73\mu_B$ for the V^{4+} ion) is equal[8] to the value reported for $BaVS_3-\delta$ with $\delta=0.05$, which confirms that La doping induces a similar electron doping effect. Applied magnetic fields H up to 3 T in 0.1-T steps were used for the isothermal magnetization curves. The internal field was determined by taking into account demagnetization effects.

III. RESULTS AND DATA ANALYSIS

The investigation of the critical behavior near T_C was carried out by means of standard methods derived from scaling theory. We recall that the three critical exponents and amplitudes of a ferro-paramagnetic phase transition are defined as follows:

$$M(H) = DH^{1/\delta} \quad \epsilon = 0,$$

$$M_s(\epsilon) = m_{0_{eff}}|\epsilon|^{\beta_{eff}} \quad \epsilon \lesssim 0,\ H = 0,$$

$$\chi_0^{-1}(\epsilon) = (h_0/m_0)_{eff}|\epsilon|^{\gamma_{eff}} \quad \epsilon \gtrsim 0,\ H = 0, \tag{1}$$

where M_s is the spontaneous magnetization, χ_0 is the magnetic susceptibility in the $H=0$ limit, and ϵ is the reduced temperature $\epsilon=(T-T_C)/T_C$, which is restricted to the critical region (typically $|\epsilon| \lesssim 0.05$). Subscripts in Eqs. (1) point out that quantities obtained from single power laws are nothing but *effective* values. True *asymptotic* values, which are meaningful with respect to the universality class of the system, can be obtained including the "correction to scaling" (CTS) terms predicted by renormalization-group (RG) theories.[15] When only the leading CTS terms are retained, the expressions for M_s and χ_0 are modified as

$$M_s(\epsilon) = m_0|\epsilon|^{\beta}(1 + a_{M_1}^{-}|\epsilon|^{\Delta_1} + a_{M_2}^{-}|\epsilon|^{\Delta_2}),$$

$$\chi_0^{-1}(\epsilon) = h_0/m_0|\epsilon|^{\gamma}(1 + a_{\chi_1}^{+}|\epsilon|^{\Delta_1} + a_{\chi_2}^{+}|\epsilon|^{\Delta_2})^{-1}. \tag{2}$$

The CTS exponent Δ_1 in Eqs. (2) is associated with quenched disorder, while Δ_2 is present both in disordered and pure ordered crystalline ferromagnets. The best available estimates for the CTS exponents are[15] $\Delta_1=0.11$ and $\Delta_2=0.55$.

The zero-field curves $M_s(T)$ and $\chi_0(T)$ in Eqs. (1) and (2) can be obtained extrapolating the isothermal magnetization curves $M(H)$ in the critical region $T \simeq T_C$ using standard methods based on the modified Arrot plots.[16] In brief, the set of $M^{1/\beta_{eff}}$ curves are plotted as a function of $(H/M)^{1/\gamma_{eff}}$ at different temperatures by varying the β_{eff} and γ_{eff} parameters, until the curves behave as predicted by the second and third ones of Eqs. (1), i.e., a series of parallel straight lines. The line passing through the origin corresponds to the critical point $T=T_C$. Using this method, we obtained $\beta_{eff}=0.507$ and $\gamma_{eff}=1.379$ (see Fig. 2). Only the points in $0.1T<H<1.3T$ were analyzed, because Arrot plots deviate from linearity outside from that range: deviation from linearity at low fields arises from mutually disaligned magnetic domains,[17] while the origin of deviation at high fields is still

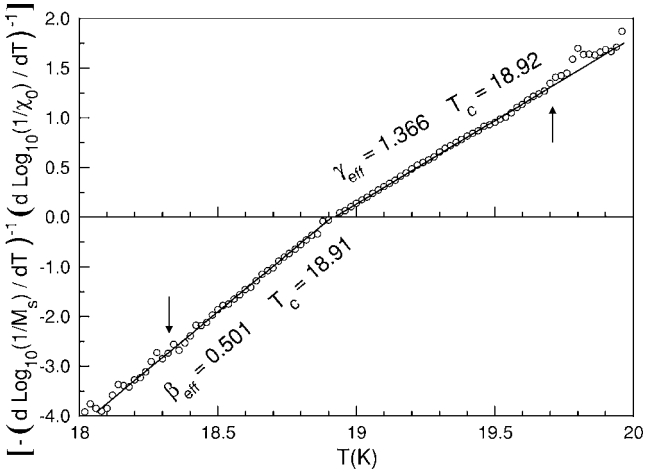

FIG. 3. Kouvel-Fisher plots of M_s and χ_0. The inverse of slopes give $\beta_{eff}=0.501$ and $\gamma_{eff}=1.366$, the intercepts on the T axis give $18.91<T_C<18.92$ K. Arrows mark the temperature range used for linear best fits.

not clear. The isotherm passing through the origin gives $T_C=18.92$ K. At this point, one can obtain $M_s(T)$ and $\chi_0(T)$ simply by extrapolating the points in Fig. 2 to the vertical and horizontal axes. The two intercepts yield, respectively, $M_s(T)$ and $\chi_0^{-1}(T)$.

In order to check the so obtained $M_s(T)$ and $\chi_0^{-1}(T)$, we applied the well-known Kouvel-Fisher method:[18] from a simple algebraic analysis of Eqs. (1), one can see that plotting $[d\log_{10}(1/M_s)/dT]^{-1}$ and $[d\log_{10}(1/\chi_0)/dT]^{-1}$ as functions of T, two straight lines that intercept the horizontal axis at $T=T_C$ with slopes $1/\beta_{eff}$ and $1/\gamma_{eff}$, respectively, should be obtained. The data analysis shown in Fig. 3 indicates that the predicted behavior is followed with $\beta_{eff}=0.501$, $\gamma_{eff}=1.366$, and $T_C\simeq 18.92$ K.

In opposition to β_{eff} and γ_{eff}, which in general depend on the analyzed temperature range, the parameters β, γ, m_0, h_0/m_0, $a^-_{M_1}$, $a^+_{\chi_1}$, $a^-_{M_2}$, and $a^+_{\chi_2}$ should result to be independent on the temperature range when this is close enough to T_C. To obtain the asymptotic critical exponents and amplitudes, we performed nonlinear least-square best fits of $M_s(T)$ and $\chi_0^{-1}(T)$ according to Eqs. (2), leaving the CTS exponents fixed at their theoretical values $\Delta_1=0.11$ and $\Delta_2=0.55$ and exploring three alternative strategies: (i) perform a best fit without the Δ_2 term, then repeat the best fit with the complete Eqs. (2) where the $a^-_{M_1}$ and $a^+_{\chi_1}$ term are frozen at the previously obtained values (this is the strategy outlined in Ref. 15); (ii) perform the best fit without the Δ_1 term; (iii) perform the best fit without the Δ_2 term. The best results (see Table I) were obtained by (iii), with fairly constant values for all of the parameters over the whole analyzed range of temperatures. Strategy (i) gives similar chi-squared values as (iii), with the appearance of oscillations of the obtained values for the fitting parameters: this is a clear symptom of an underdetermined problem, i.e., too many free parameters. (ii) gives higher chi-squared values than (iii), and less stable values for the fitting parameters. This could be explained if the measured range of temperatures were too close to T_C, since $\Delta_1<\Delta_2$ implies that the Δ_1 prevails over the Δ_2 term when ϵ is very small. Nevertheless, a range of $\epsilon\simeq 5\%$ is usually far enough to let the Δ_2 term show up. We suggest that the fact that the CTS exponent Δ_1 turns out to be definitively more important than Δ_2 could be ascribed to the disorder in the local demagnetizing factors of the single grains in our dry pressed powder sample.

According to the first one of Eqs. (1), the exponent δ can be obtained from the isothermal magnetization curves $M(H)$ in the critical region $T\simeq T_C$, namely the slope of the magnetization curve at the critical temperature equals $1/\delta$ when plotted on logarithmic scale. This gives also an alternative way to determine the value of T_C. The application of this method to our data yields $T_C=19.00$ K and $\delta=3.640$ (Fig. 4).

The reliability of the obtained values of the critical exponents and T_C can be checked by means of a scaling analysis. According to the scaling hypothesis,[19,20] the singular part of

TABLE I. Critical exponents and amplitudes, and T_C obtained from magnetization data on $La_{0.1}Ba_{0.9}VS_3$, and predicted values for the three-dimensional Heisenberg (H3D), *XY* (*XY*3D), mean-field theory (MFT), and Ising (IS3D) models. Numbers in the parentheses denote the uncertainty in the least significant figure arising from the different methods of analysis.

Method[a]	β	ϵ range for fit (10^{-3})	γ	ϵ range for fit (10^{-3})	δ	T_C (K)	$a^-_{M_1}$	m_0 (emu/g)	$a^+_{\chi_1}$	m_0/h_0 (g Oe/emu)
AP	0.507	49	1.379	53	3.719[b]	18.92				
KF$^-$	0.501(10)	9–49			3.726(130)[b]	18.91		7.65(34)		
KF$^+$			1.366(36)	6–43	3.726(130)[b]	18.92				5.4(6) 10^{-5}
CTS$^-$	0.519(2)	<1–47			3.663(30)[b]	18.92	−0.16(2)	8.9(2)		
CTS$^+$			1.382(10)	3–56	3.663(30)[b]	18.91			0.26(10)	4.4(4) 10^{-5}
MH					3.640	19.00				
H3D (Ref. 23)	0.364		1.386		4.80[b]					
*XY*3D (Ref. 23)	0.345		1.316		4.80[b]					
IS3D (Ref. 23)	0.325		1.241		4.82[b]					
MFT (Ref. 24)	0.5		1.0		3.0					

[a]AP: Arrot plots; KF: Kouvel-Fisher; CTS: correction to scaling; MH: $\log_{10}(M)$ vs $\log_{10}(H)$.
[b]Calculated values $\delta=(\beta+\gamma)/\beta$.

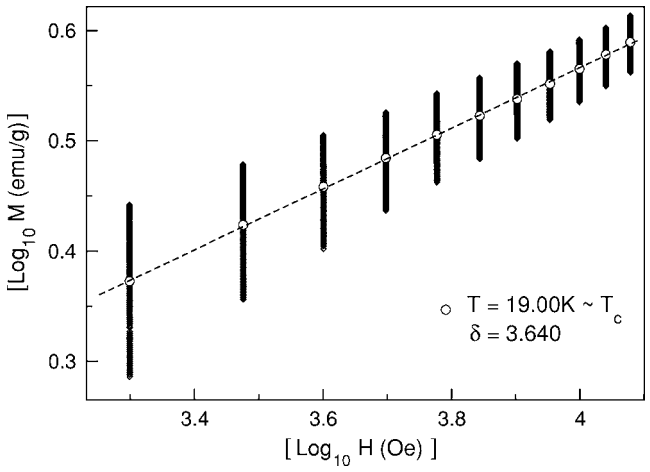

FIG. 4. Isothermal magnetization curves in the $18.00 \leqslant T \leqslant 20.00$-K interval. Temperature steps are $\Delta T = 0.02$ K.

the Gibbs potential per spin is a generalized homogeneous function of H and of the reduced temperature ϵ. Under this assumption, for any positive number, λ, there exist two numbers, a and b, satisfying the relation $G(\lambda^a H, \lambda^b \epsilon) = \lambda G(H, \epsilon)$. This assumption leads to two important consequences: (i) the critical exponents are not independent, for they are linked by the relation $\beta\delta = \beta + \gamma$; (ii) in a ferromagnetic phase transition, the following universal equation of state holds: $\frac{M(H,\epsilon)}{|\epsilon|^\beta} = f_\pm\left(\frac{H}{|\epsilon|^{\beta\delta}}\right)$. According to the above two relations, the experimental $M(H)$ curves are expected to collapse into the universal curve $M(H,\epsilon)/|\epsilon|^\beta = f_\pm(H/|\epsilon|^{\beta\delta})$ for the two branches of positive and negative reduced temperature ϵ, by plotting the experimental data as $\log_{10}(H/\epsilon^{\beta\delta})$ as a function of $\log_{10}(M/\epsilon^\beta)$. Although it has been shown that the above scaling analysis cannot be used to directly determine the critical exponents,[21] it is commonly accepted as a valid backward test of internal consistency for the critical exponent values estimated by means of other methods, as in our case. In Fig. 5 the scaled experimental points for $\beta = 0.519$, $\gamma = 1.382$, $T_C = 18.92$ K are shown, and one easily notes that the scaling hypothesis leading to the aforementioned two branches of universal curve for $\epsilon > 0$ and $\epsilon < 0$ is well satisfied.

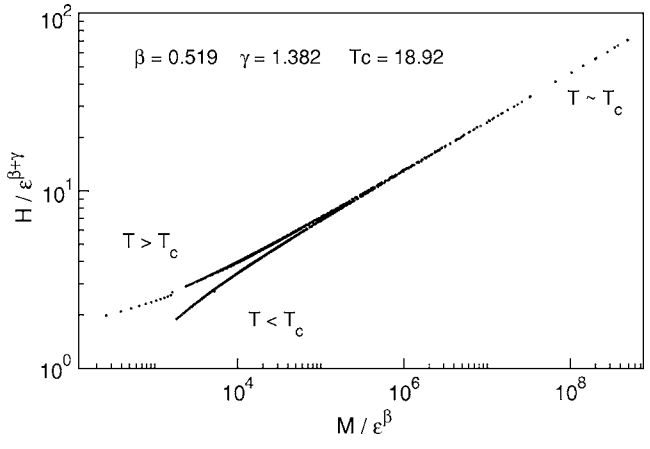

FIG. 5. Logarithmic scaling plot of $H/\epsilon^{\beta+\gamma}$ vs M/ϵ^β in the critical region. The experimental points fall on two branches of a universal curve by using the values of the critical exponents and of T_C obtained by means of CTS analysis. The points on the isotherm at T_C have diverging coordinates and are not reported.

TABLE II. Critical amplitude ratios for $La_{0.1}Ba_{0.9}VS_3$, and predicted values for the three-dimensional Heisenberg (H3D), mean-field theory (MFT), and Ising (IS3D) models.

	$M_S(0)$ (emu/g)	μ_0 (μ_B)	$m_0/M_S(0)$	$\mu_0 h_0/k_B T_C$
KF	5.15	0.27	1.48	0.12
CTS	5.20	0.27	1.71	0.19
H3D (Ref. 22)			1.37	1.58
IS3D (Ref. 25)			1.49	1.52
MFT (Refs. 25 and 26)			1.73	1.73

As for critical amplitudes, according to theory the ratios $m_0/M_S(0)$ (for $T < T_C$) and $\mu_0 h_0/k_B T_C$ (for $T > T_C$), where $M_S(0)$ and μ_0 are the spontaneous magnetization and the magnetic moment per V atom at $T = 0$ K, should have definite values, depending on the universality class of the system. In order to estimate $M_S(0)$, we performed an $M(H)$ magnetization measurement at $T = 5$ K and considered the linear part of the modified Arrot plots resulting from the previously obtained values of β and γ. In Table II we compare the values obtained from our analysis with those computed for some universality classes.

The results show that Kouvel-Fisher and CTS analysis give consistent results, with smaller uncertainties and far better chi-squared values in the case of the latter (note the logarithmic scale in Fig. 6). Magnetic interactions in our $La_{0.1}Ba_{0.9}VS_3$ exhibit to two different behaviors above and below T_C: below T_C the critical exponent $\beta = 0.519$ indicates long-range magnetic interaction, while above T_C the critical exponent $\gamma = 1.382$ indicates local magnetic interaction (Table I). This point is corroborated by the critical amplitude ratio $m_0/M_S(0)$ reported in Table II, which is more compat-

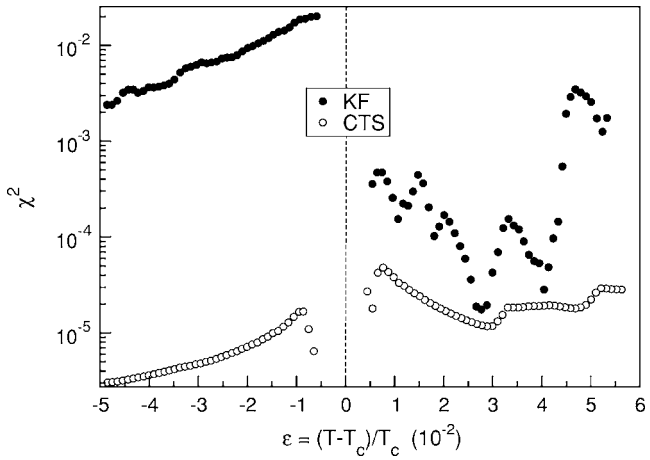

FIG. 6. Values of χ^2 for best fits resulting from Kouvel-Fisher method and CTS analysis plotted as function of reduced temperature. $\chi^2 = 1/(N - N_p)\Sigma_i[(y_{fit} - y_{exp})/y_{exp}]^2$ where N is the number of data points and N_p is the number of free fitting parameters.

ible with the MFT model than with short-range interactions. The reduced value of μ_0 supports the hypothesis, as already suggested for sulfur deficient $BaVS_{3-\delta}$ compounds,[8] of the appearance of a spin-singlet phase below T_C in coexistence with the magnetic phase, which would account for the reduced magnetic moment observed in the ordered state.

IV. CONCLUSION

We have obtained the critical exponents and amplitudes for the magnetic transition of $La_{0.1}Ba_{0.9}VS_3$ by means of CTS analysis. The results correspond to two different universality classes on the two sides of the magnetic transition therefore suggesting a change in the nature of magnetic interactions when crossing the transition point, passing from short-range order to long-range order on cooling through T_C. The universality class for the $T>T_C$ phase is in agreement with the results of DFT calculations,[13] while the change in the universality class can probably be associated to the charge-ordering structural transition.[14] It is worth reminding that a similar behavior had been previously reported for sulfur deficient $BaVS_{3-\delta}$ by means of ^{51}V NMR studies,[8] and was explained as a transition from an antiferromagnetic insulator to a ferromagnetic metal. The common feature to the two compound classes promoting ferromagnetic short-range order can be identified in the extra electron on the Vt_{2g} orbital, which couples different *ab* planes through Hund interaction. In this frame, it would be interesting to study how the magnetic transition properties evolve with respect to the amount of electron doping x in electron doped $La_xBa_{1-x}VS_3$.

*Electronic address: cabassi@imem.cnr.it

[1] See, for example, Yu. M. Ivanchenko and A. A. Lisyansky, in *Physics of Critical Fluctuations* (Springer, New York, 1995).
[2] R. Gardner, M. Vlasse, and A. Wold, Acta Crystallogr., Sect. B: Struct. Crystallogr. Cryst. Chem. **25**, 781 (1969).
[3] L. Forro, R. Gaal, H. Berger, P. Fazekas, K. Penc, I. Kezsmarki, and G. Mihaly, Phys. Rev. Lett. **85**, 1938 (2000).
[4] G. Mihaly, I. Kezsmarki, F. Zamborszky, M. Miljak, K. Penc, P. Fazekas, H. Berger, and L. Forro, Phys. Rev. B **61**, R7831 (2000).
[5] H. Nakamura, H. Tanahashia, H. Imai, M. Shigaa, K. Kojimab, K. Kakuraic, and M. Nishi, J. Phys. Chem. Solids **60**, 1137 (1999).
[6] H. Nakamura, T. Yamasaki, S. Giri, H. Imai, M. Shiga, K. Kojima, M. Nishi, K. Kakurai, and N. Metoki, J. Phys. Soc. Jpn. **69**, 2763 (2000).
[7] O. Massenet, R. Buder, J. J. Since, C. Schlenker, and J. Mercier, Mater. Res. Bull. **13**, 187 (1978).
[8] T. Yamasaki, H. Nakamura, and M. Shiga, J. Phys. Soc. Jpn. **69**, 3068 (2000).
[9] T. Inami, K. Ohwada, H. Kimura, M. Watanabe, Y. Noda, H. Nakamura, T. Yamasaki, M. Shiga, N. Ikeda, and Y. Murakami, Phys. Rev. B **66**, 073108 (2002).
[10] S. Fagot, P. Foury-Leylekian, S. Ravy, J.-P. Pouget, and H. Berger, Phys. Rev. Lett. **90**, 196401 (2003).
[11] L. F. Mattheiss, Solid State Commun. **93**, 791 (1995).
[12] M. H. Whangbo, H. J. Koo, D. Dai, and A. Villesuzanne, J. Solid State Chem. **175**, 384 (2003).
[13] Xuefan Jiang and G. Y. Guo, Phys. Rev. B **70**, 035110 (2004).
[14] S. Fagot, P. Foury-Leylekian, S. Ravy, J.-P. Pouget, M. Anne, G. Popov, M. V. Lobanov, and M. Greenblatt, Solid State Sci. **7**, 718 (2005).
[15] P. D. Babu and S. N. Kaul, J. Phys.: Condens. Matter **9**, 7189 (1997), and references therein.
[16] A. Arrot and J. E. Noakes, Phys. Rev. Lett. **19**, 786 (1967).
[17] A. Aharony, *Introduction to the Theory of Ferromagnetism* (Clarendon, Oxford, 1996).
[18] J. S. Kouvel and M. E. Fisher, Phys. Rev. **136**, 1626 (1964).
[19] H. E. Stanley, *Phase Transitions and Critical Phenomena* (Clarendon, Oxford, 1971).
[20] H. E. Stanley, Rev. Mod. Phys. **71**, S358 (1999).
[21] M. Fähnle, W. U. Kellner, and H. Kronmüller, Phys. Rev. B **35**, 3640 (1987).
[22] S. N. Kaul, J. Magn. Magn. Mater. **53**, 5 (1985).
[23] J. C. Le Guillou and J. Zinn-Justin, Phys. Rev. B **21**, 3976 (1980).
[24] V. L. Ginzburg and L. D. Landau, Zh. Eksp. Teor. Fiz. **20**, 1064 (1950).
[25] S. N. Kaul, Phys. Rev. B **24**, 6550 (1981).
[26] M. Nakamura, A. Sekiyama, H. Namatame, A. Fujimori, H. Yoshihara, T. Ohtani, A. Misu, and M. Takano, Phys. Rev. B **49**, 16191 (1994).